



## RESEARCH LETTER

10.1002/2014GL059562

## Key Points:

- Multimodels show a robust spring drying in southwestern U.S.
- Water availability changes follow north-south and east-west dipole patterns
- Seasonal migration of wet/dry patterns in the U.S.

## Supporting Information:

- Readme
- Text S1
- Figure S1
- Figure S2
- Figure S3
- Figure S4
- Figure S5
- Figure S6

## Correspondence to:

L. R. Leung,  
Ruby.Leung@pnnl.gov

## Citation:

Gao, Y., L. R. Leung, J. Lu, Y. Liu, M. Huang, and Y. Qian (2014), Robust spring drying in the southwestern U.S. and seasonal migration of wet/dry patterns in a warmer climate, *Geophys. Res. Lett.*, 41, doi:10.1002/2014GL059562.

Received 10 FEB 2014

Accepted 21 FEB 2014

Accepted article online 25 FEB 2014

## Robust spring drying in the southwestern U.S. and seasonal migration of wet/dry patterns in a warmer climate

Yang Gao<sup>1</sup>, L. Ruby Leung<sup>1</sup>, Jian Lu<sup>1</sup>, Ying Liu<sup>1</sup>, Maoyi Huang<sup>1</sup>, and Yun Qian<sup>1</sup>

<sup>1</sup>Atmospheric Sciences and Global Change Division, Pacific Northwest National Laboratory, Richland, Washington, USA

**Abstract** This study compares climate simulations over North America produced by a regional climate model with the driving global climate simulations as well as a multimodel ensemble of global climate simulations to investigate robust changes in water availability (precipitation (P)-evapotranspiration (E)). A robust spring-drying signal across multiple models is identified in the Southwest that results from a decrease in P and an increase in E in the future. In the boreal winter and summer, the prominent changes in P-E are associated with a north-south dipole pattern, while in spring, the prominent changes in P-E appear as an east-west dipole pattern. The progression of the north-south and east-west dipole patterns through the seasons manifests clearly as a seasonal “clockwise” migration of wet/dry patterns, which is a robust feature of water availability changes in North America consistent across regional and global climate simulations.

### 1. Introduction

Global climate models (GCMs) used in the Coupled Model Intercomparison Project Phase 3 (CMIP3) and Phase 5 (CMIP5) [Taylor *et al.*, 2012] have projected changes in precipitation characteristics in a warmer climate. In a series of studies, Seager *et al.* [2007, 2013] and Seager and Vecchi [2010] reported a long-term decline of water availability from the CMIP3 and CMIP5 simulations over the southwestern U.S. in the future. Because GCMs lack spatial specificity to capture finer-scale orographic processes that dominantly control the hydrologic cycle in the western U.S., regional climate models (RCMs) have been used to examine differences in climate change signals that may be attributed to regional processes simulated at different model resolutions [Leung and Ghan, 1999; Leung *et al.*, 2004]. Gao *et al.* [2012] analyzed four pairs of GCM-RCM simulations over the southwestern U.S. and found that RCMs generally projected reduced future drying compared to the GCM counterparts. They suggested that increased atmospheric static stability in a warmer climate might enhance transient eddies moisture convergence on the windward slopes of the mountains, which counters the drying due to the mean divergent circulation. Using a larger ensemble of GCM-RCM simulations from the North American Regional Climate Change Assessment Program (NARCCAP), however, Mearns *et al.* [2013] did not find a consistent difference between GCM and RCM projected future drying over the Southwest.

Although RCMs can provide more spatially detailed simulations of regional climate for assessing climate change impacts, they require significant computational resources, so RCM simulations are commonly performed using a single model in time slice experiments. NARCCAP used an ensemble of RCMs and GCMs in a balanced nested design. Still only four GCMs were used so uncertainties in regional climate changes due to uncertainties in the large-scale changes projected by the GCMs remain. Furthermore, the RCM simulations were performed at a relatively coarse spatial resolution of 50 km [Mearns *et al.*, 2012] that still under represent the substantial spatial heterogeneity of the U.S. climate, and downscaling was performed only for two 30 year periods of 1970–2000 and 2040–2070, although projections for the near term and century scale are both important for climate adaptation and mitigation research.

This study compares long-term simulations by a regional climate model at a relatively high spatial resolution of 20 km over North America with the GCM simulations that provided boundary conditions as well as a multimodel ensemble of simulations from CMIP5 on the century time scale. We examine how representative climate change signals from high-resolution simulations generated by a single RCM and its GCM counterpart are in the context of a large multimodel GCM ensemble. Our goal is to identify robust changes across models and the associated large-scale circulation changes so that future analysis can focus on those features to elucidate the role of regional processes in modulating those climate changes. Our analysis focuses on robust

broad-scale features of water availability changes in North America. We define water availability as the difference between precipitation (P) and evapotranspiration (E), or P-E, which corresponds to the terrestrial water available in the form of runoff, soil moisture, snowpack, and groundwater. Both model agreement and statistical significance are used to identify robust changes across the regional and global simulations. Section 2 describes the models and simulations used in the analysis and comparison of the simulation with observation data. This is followed by analysis of annual and seasonal changes in water availability in section 3, relationships between the water availability changes and large-scale circulation changes in section 4, and seasonal progression of water availability changes in section 5. Lastly, the study is summarized in section 6.

## 2. Model Description and Evaluation

The Weather Research and Forecasting (WRF) model version 3.2 [Skamarock *et al.*, 2008] coupled with the Community Land Model [Oleson *et al.*, 2010; Ke *et al.*, 2012] was used to dynamically downscale a single member of historical climate (1975–2004) and two scenarios of future climate (2005–2100) simulated by the Community Climate System Model version 4 (CCSM4) [Gent *et al.*, 2011] at 0.9° (latitude) by 1.25° (longitude) resolution as part of the CMIP5 archive. The WRF model was applied at a horizontal resolution of 20 km over North America. In addition, model outputs from 20 CMIP5 models with a total of 30 ensemble members are used. The CMIP5 models are summarized in Table S1 in the supporting information. We examined two RCP scenarios for the low-to-medium emission scenario RCP4.5 and fossil fuel intensive scenario RCP8.5 [Moss *et al.*, 2010; van Vuuren *et al.*, 2011]. To evaluate the WRF and CCSM4 simulations, model outputs have been compared with observed daily precipitation data [Maurer *et al.*, 2002] for the historical period (1975–2004). The models show good agreement with observations of precipitation, evapotranspiration, 500 hPa geopotential height, and frequency distributions of precipitation in 12 major river basins. More details on the WRF configuration and model evaluation are provided in Text S1 in the supporting information and Figures S1–S4.

## 3. Seasonal Changes of P-E in the Multimodel Ensemble

Figure 1 compares the mean annual and seasonal changes of P-E in the future (2070–2099) with the present (1975–2004) from WRF, CCSM4, and the CMIP5 ensemble mean in North America. Grid cells with statistically significant changes are marked in Figure 1 (red dots) for WRF and CCSM4. For CMIP5, we compare two methods to depict multimodel results based on (1) model agreement on the sign of the change only [Seager *et al.*, 2013] and (2) both statistical significance of the change and model agreement on the sign of the change [Tebaldi *et al.*, 2011]. Unlike Tebaldi *et al.* [2011] that used only one ensemble member from each model, we take advantage of all ensemble members and tested all members of each model for statistically significant changes. If at least half of the members show statistical significance, that model is considered to simulate statistically significant changes.

Comparing WRF with CCSM4, the P-E changes are generally consistent with the main exception of a wet trend over the Atlantic coast in CCSM4 in summer, which is absent in WRF. The regional simulations also show more spatially resolved changes associated with topography and coastline, which will be analyzed in more detail in a follow-on study. Some robust large-scale changes in P-E are apparent for each season across WRF, CCSM4, and the CMIP5 multimodel ensemble. The most robust drying in the future occurs in spring over the Southwest, followed by drying in New Mexico, Texas, and northern Mexico in winter, and Northwest in summer. Pierce *et al.* [2013] also noted a reduction in spring precipitation in California from analysis of climate change signals in CMIP5 and dynamically and statistically downscaled scenarios. Areas with robust wet trends occur in small areas of the Northeast and Northwest in winter, and in the Southwest and Texas in summer. Although WRF and CCSM4 simulated statistically significant wet trends in California during winter, the changes in the CMIP5 ensemble are neither statistically significant nor show model agreement. Most of the changes in the fall are either not statistically significant or inconsistent across models. Comparing Figure 1 (third and fourth panels), areas with both statistical significance and model agreement are smaller than areas with model agreement only, indicating that model agreement is not always coincident with statistical significance. On annual scale, very few grid cells show consistency as well as statistical significance.

To further elucidate the robust dry and wet patterns that occur in spring, time series of spring P-E from WRF, CCSM4, and the CMIP5 median in Figure S5 in the supporting information show consistent long-term

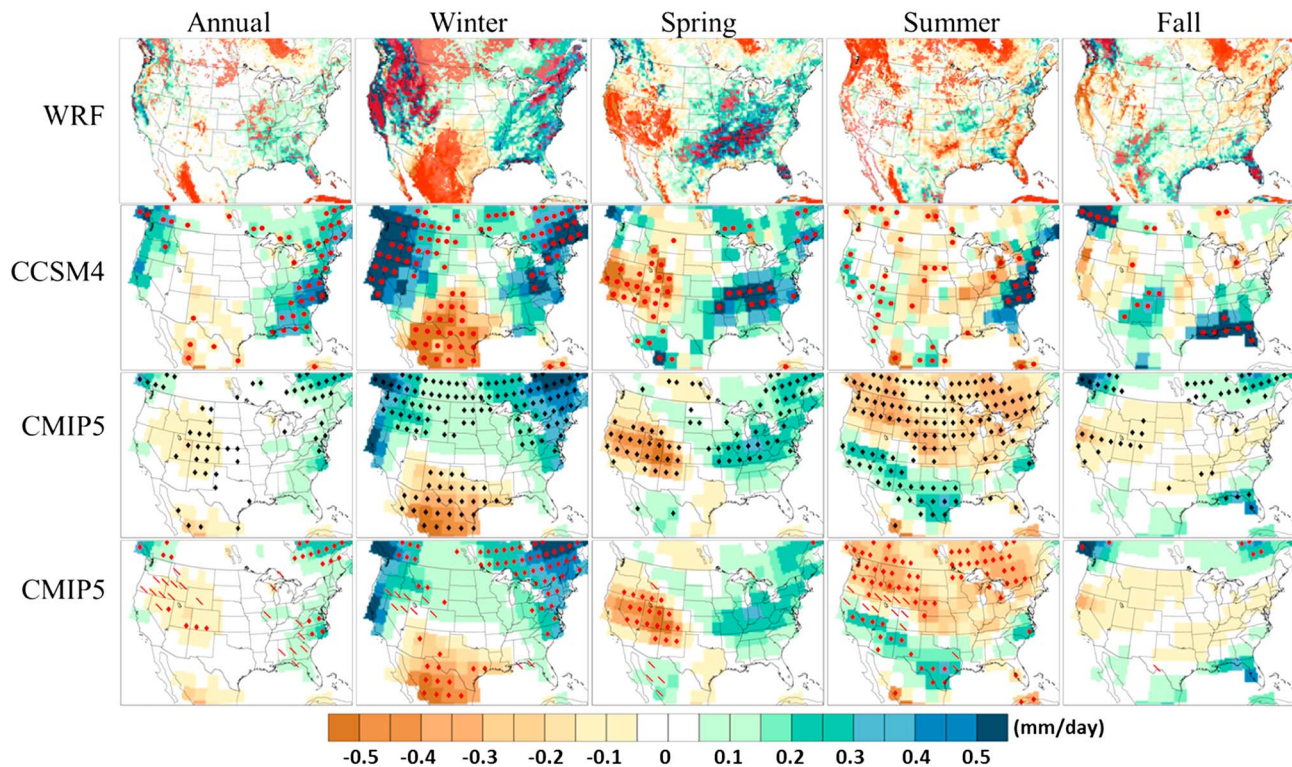


**Figure 1.** Changes of P-E comparing 2070–2099 to 1975–2004 under RCP8.5: (first and second panels) red stippled areas indicate changes with statistical significance; (third panel) black diamond indicates 75% of CMIP5 models agree with the CMIP5 mean on the sign of the change; (fourth panel) for grids with at least 50% of CMIP5 models showing statistical significant changes in the future, areas with more (less) than 80% of the models agree with sign of the CMIP5 mean change are marked by red dots (red hatch).

decreasing trends of P-E in the California-Nevada and Colorado Basins and wet trends in Ohio Basin and the Southeast from 1975 to 2100. The century-scale trends are consistent with the 30 year mean change patterns shown in Figure 1. Comparing the relative contributions of P and E to P-E changes, time series of CMIP5 median P, E, and P-E spring changes in Figure S6 show small increases in E while P drops dramatically, thus driving significant decrease of P-E in the Southwest. In the Ohio Basin and the Southeast, the wet trends are mainly contributed by the larger increase of P, overcoming the small increase in E. Hence, the CMIP5 models as well as WRF and CCSM4 (not shown) all indicate that warming in the future drives an increase in evaporative demand that contributes to drying over land.

#### 4. Relationship Between Circulation and P-E Changes

The broad features of P-E changes may be related to dynamical changes associated with changes in the mean large-scale circulation and transient storm tracks or thermodynamical changes associated with increases in atmospheric water vapor in a warmer climate. To provide insights on their potential roles in changing P-E, Figure 2a shows the changes in 500 hPa geopotential height (GHT) comparing 2070–2099 to 1975–2004 for winter and summer simulated by WRF under RCP8.5, with similar changes for RCP4.5 and from CCSM4 and CMIP5 mean (not shown). The winter mean GHT change pattern resembles the Aleutian low pressure system typically found over the Gulf of Alaska and indicates a deepening of the low pressure center in the future. During summer, an enhanced ridge extends from the Arctic to the Pacific Northwest.

To determine the extent to which the hydrological response can be explained by the local and upstream mean circulation changes, we first project the time series of the detrended seasonal anomalies of GHT from 1975 to 2099 onto the GHT change pattern. The resulting time index represents the interannual fluctuation of the GHT change pattern. Regressing the P-E anomalies for the same time period against the time index of the GHT change pattern yields its hydrological impact. For winter, the regression pattern of P-E (Figure 2c, left) shows considerable resemblance to the simulated P-E change pattern (Figure 2b, left), with a spatial

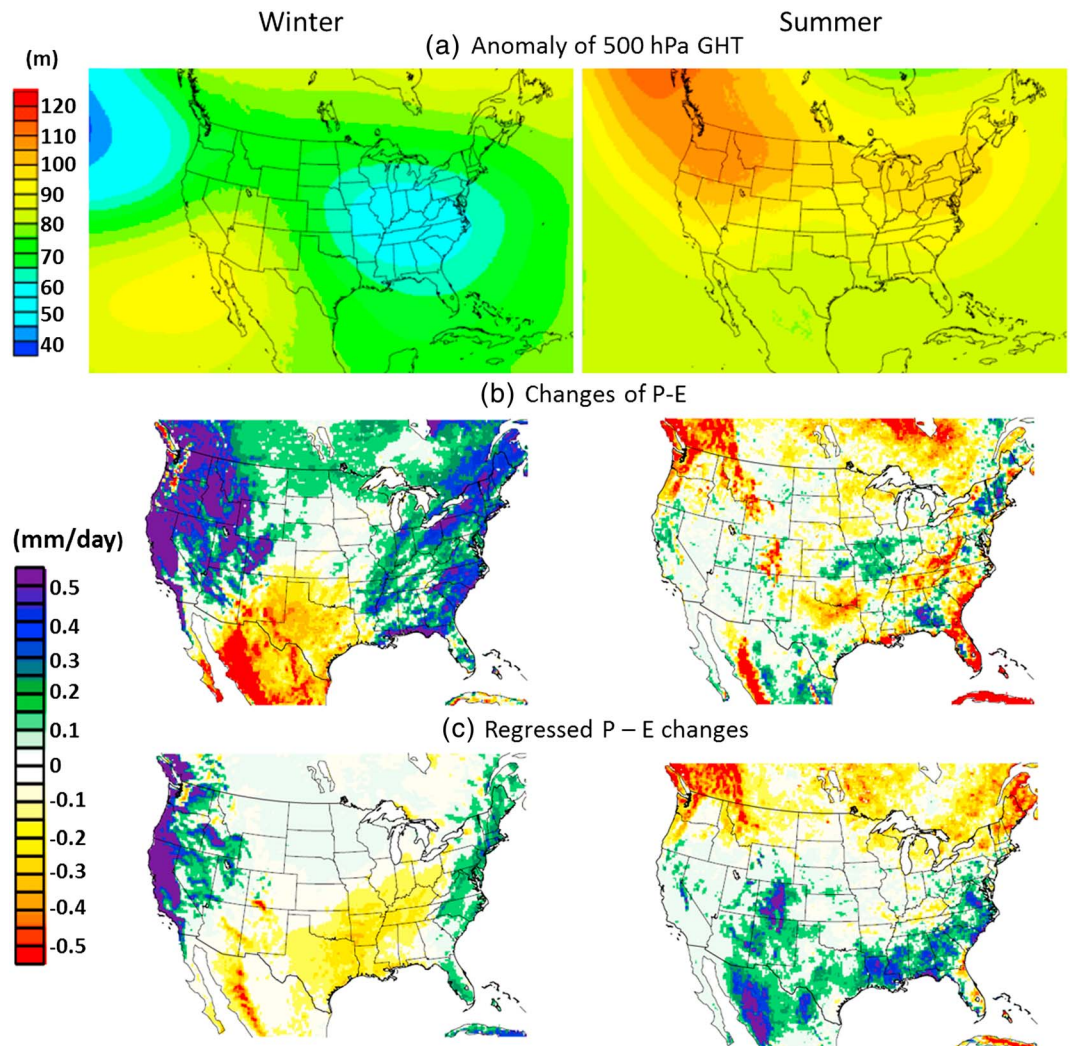


**Figure 2.** Mean changes in (a) 500 hPa geopotential height (GHT) (in meter) and (b) P-E (in mm/d) for winter (left) and summer (right) simulated by WRF comparing the future (2070–2099) with the present (1975–2004). (c) Regression of P-E changes onto the 500 hPa GHT changes.

correlation of 0.54 over the conterminous U.S., 0.91 in the California-Nevada Basin, and 0.64 in the Colorado Basin. This suggests that some of the increasing winter P-E trend in the west coast, and to some extent the drying in the Southwest, can be attributed to the mean GHT changes. Hence, the enhanced winter P-E in the western U.S. is partly related to the increased moisture convergence associated with the stronger mean southwesterly flow on the southeast flank of the Aleutian low that advects more moisture to the west coast. Increased moisture associated with warming would also contribute to the increased moisture convergence.

During the boreal winter, the increase in tropopause height [Lorenz and DeWeaver, 2007] and changes in baroclinicity [Frierson et al., 2007; Lu et al., 2008] can lead to a strengthening and poleward shift in the zonal jet upstream of the North Pacific storm track. However, using Lagrangian tracking and variance statistics calculated from the CMIP5 simulations, Chang et al. [2012] found no systematic shift but an overall weakening of storm tracks over North America. Thus, the contribution of transient storms to the increase of winter P-E in the western U.S. is likely inconsequential, a notion that is yet to be verified with quantitative analysis such as atmospheric moisture budget [e.g., Seager and Vecchi, 2010]. The 200 hPa zonal winds from the CMIP5 simulations also show little change in the mean location of the jet stream (Figure 3). Instead, there is an eastward extension of the jet stream that slightly veers northeast near the West Coast, which may steer more moisture toward the coastal mountains and enhance orographic precipitation in the future [Neelin et al., 2013].

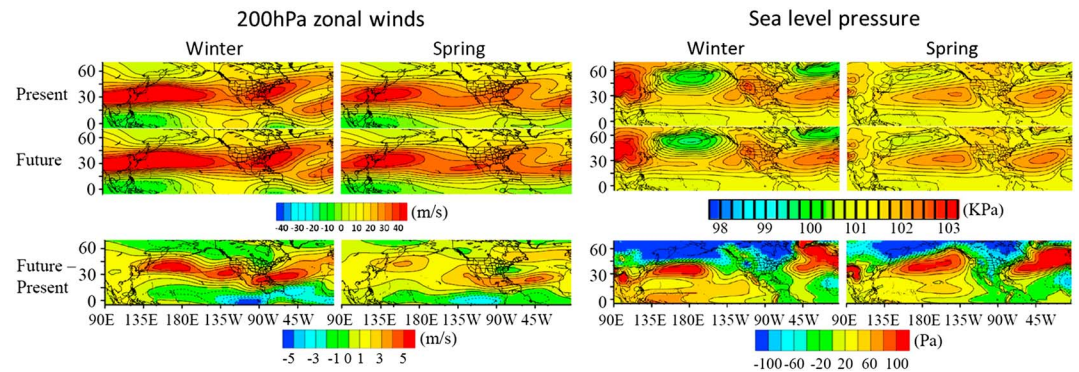


**Figure 3.** (left) Mean 200 hPa zonal winds in m/s for present (1975–2004), future (2070–2099), and future–present for winter and spring from the CMIP5 ensemble mean for RCP8.5. (right) Similar to the left but for sea level pressure.

However, Figure 1 (fourth panel) indicates no consensus on the winter moistening trend in the western U.S. (despite its statistical significance) among the CMIP5 models. This is consistent with the uncertainty in the sign or magnitude of the projected circulation changes.

Applying the same regression analysis of GHT and P-E changes to the summer, the high pressure with a southeastward intrusion contributes to drying over the Pacific Northwest, with the spatial correlation between the simulated and regressed P-E change patterns reaching 0.86. Despite the most robust and significant projection of spring drying in the southwestern U.S., no significant changes in the mean 500 hPa GHT or 200 hPa zonal winds (Figure 3) are found over the U.S. in WRF, CCSM4, or the CMIP5 ensemble mean. In spring, the jet stream that steers synoptic storms toward the west coast weakens and retreats to the central North Pacific. At the same time, the North Pacific and North Atlantic subtropical high-pressure centers develop and move closer to western and eastern North America, respectively (Figure 3). The strengthening and expansion of the subtropical high [Li *et al.*, 2012] is a basin-scale manifestation of the expansion of the Hadley cell [Lu *et al.*, 2007; Frierson *et al.*, 2007]. The stronger and expanded Pacific subtropical high pressure together with the increased atmospheric moisture due to warming enhances the mean moisture divergence and contributes to the drying in the Southwest in the future.

## 5. Seasonal Progression of P-E Changes

It is interesting to note in Figure 1 that the dominant regions experiencing dry and wet trends in the future change with the season. To summarize this feature in the context of the large-scale changes discussed in section 4, the seasonal shift of P-E under RCP8.5 is shown in Figure 4, and similar patterns are obtained for RCP4.5 (not shown). Only CMIP5 mean is used to describe the seasonal shift, as the regional model shows very similar broad scale feature, albeit some topographic influence at finer scales. On each grid, the month with the largest negative P-E change (i.e., largest drying) is plotted in Figures 4a and 4c, while the month with the largest positive P-E change (i.e., largest wet trend) is plotted in Figures 4b and 4d. For P-E changes comparing both 2050s and 2090s with the present, there is a spatially consistent and coherent seasonal shift for both dry and wet trends. Drying begins in winter (December, January, and February (DJF), Figure 4, blue) in New Mexico, Texas, and northern Mexico but shifts north to the Southwest (March, April, and May (MAM), Figure 4, black); it progresses further north and extends to the east in summer (June, July, August (JJA), Figure 4, red). In fall, the dry area moves slightly southeastward, although the changes are not statistically significant (Figure 1). These represent a “clockwise” shift of the dry region in North America from the southern regions in winter to the Southwest in spring and the North and Northeast in summer. The movement of the wet regions is complementary to the dry regions and follows the clockwise shift. In winter (DJF), while drying occurs in the southern regions, the North experiences a wet trend, which propagates to the East in spring (MAM), and then move to the South in summer (JJA). The changes of P-E under RCP4.5 show similar seasonal shifts (not shown).

The seasonal shift and clockwise propagation of the dry and wet regions are reflections of the dominant large-scale controls of P-E through the seasons. During the boreal winter, although the contributions of storm

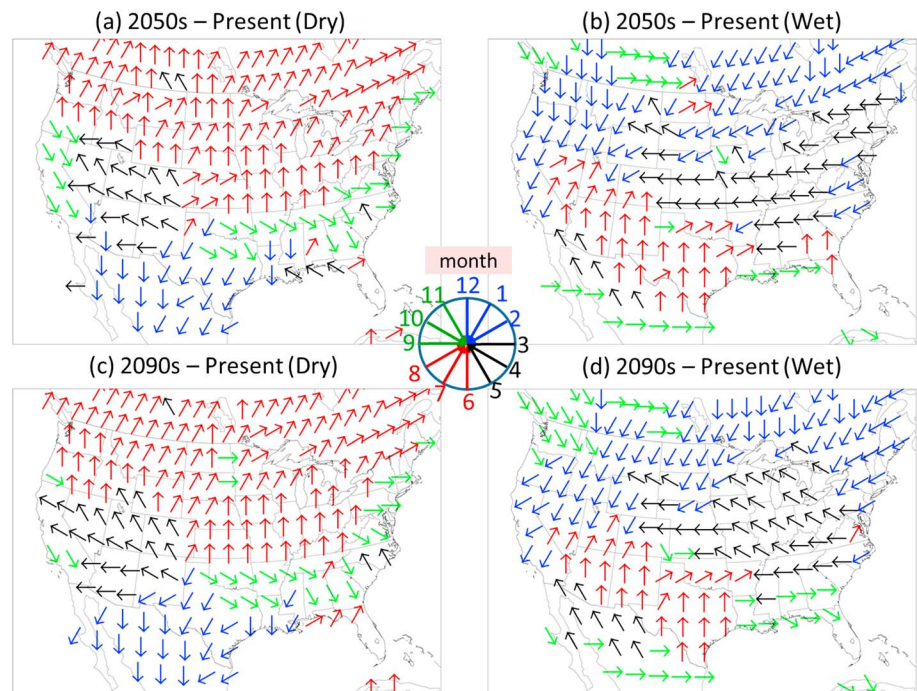


**Figure 4.** Seasonal shift of the timing of maximum (a, c) negative and (b, d) positive P-E changes from the CMIP5 ensemble mean under RCP8.5 comparing the 2050s (Figures 4a and 4b) and 2090s (Figures 4c and 4d) with the present. The month for the maximum change at each grid cell is shown by the direction of the arrow, while the color corresponds to the season of the month.

track changes to P-E are less clear, the deepening of the Aleutian low (Figure 2) enhances precipitation roughly north of central California, leading to the dominant north-south dipole in P-E changes. During spring, the zonal jet weakens and the subtropical high pressure in the Pacific and Atlantic develops and moves toward the continent. As the high pressure centers strengthen and expand poleward (Figure 3), and moisture is enhanced in the warmer climate, the mean moisture divergence increases and dries the Southwest. In the Southeast, the strengthened subtropical high steers more moisture toward the continent and may contribute to the wet trend. Hence, the dominant P-E change is an east-west dipole in spring rather than a north-south dipole as in winter over North America. In summer, increased moisture from the Gulf of Mexico likely plays a role in increasing P-E in the South. Together with changes in the mean GHT pattern (Figure 2), the circulation changes lead to drying in the north and moistening in the South. As the large-scale circulation changes most prominently influence the midlatitude weather systems, the seasonal migration patterns are more distinctive over the conterminous U.S. Most of these changes are robustly simulated by the CMIP5 models as well as the WRF regional climate model in response to the broad-scale circulation changes.

## 6. Summary

The future prospects of water availability over North America is investigated by analysis of simulations from the CMIP5 global climate models and a high-resolution regional climate model with its boundary conditions provided by global climate simulations. Areas with statistically significant changes are compared across WRF, CCSM4, and the CMIP5 multimodel ensemble to look for model agreement. We identified a robust dry signal in the Southwest in spring that is statistically significant and consistent across the WRF, CCSM4, and CMIP5 simulations. For other seasons, using model agreement alone could result in over emphasizing P-E changes that are not statistically significant. The robust spring dry signal is related to a decrease in P as well as an increase in E, thus significantly reducing the terrestrial water storage in the Southwest during spring. On annual average, however, P-E changes show little agreement or are mostly statistically insignificant.

Summarizing the role of circulation changes in P-E changes, the model results suggest that both the winter and spring P-E changes might have a large dynamical origin, with the former from deepening of the Aleutian low pressure center and eastward extension of the westerly jet, and the latter from strengthening and

expansion of the subtropical high pressure in the Pacific and Atlantic, respectively. During summer, mean circulation changes are also found to play a role in the drying in the Pacific Northwest. Overall, the prominent changes in P-E are associated with a north-south dipole pattern related to the 500 hPa GHT and storm track changes in winter and a reversed dipole pattern associated with the 500 hPa GHT changes and enhanced moisture transport from the Gulf of Mexico in summer. In spring, the prominent changes in P-E appeared as an east-west dipole pattern related to changes in the subtropical high-pressure systems. Progression of the dominance of the north-south dipole and east-west dipole patterns through the seasons manifests as a spatially consistent and coherent seasonal (clockwise) migration of dry/wet patterns that define robust changes in water availability in the North America.

The robust seasonal P-E changes consistent across regional and global climate simulations can present important challenges for water resources management that aimed at balancing seasonal water supply and demand and for rain-fed agriculture that relies on soil moisture in spring and summer. Future analysis of subbasin-scale hydrologic changes will provide further insights on regional water availability. Numerous surface and three-dimensional variables from the WRF simulations at 20 km grid resolution have been archived at hourly to daily frequency from 1975 to 2100. The model outputs can be made available upon request for analysis and impact assessment research.

#### Acknowledgments

This study was supported by the Office of Science of the U.S. Department of Energy as part of the Integrated Assessment Research and Regional and Global Climate Modeling programs. The regional climate simulations were conducted with partial support by the Platform for Regional Integrated Modeling and Analysis (PRIMA) Initiative at Pacific Northwest National Laboratory (PNNL). The regional simulations were performed on the Evergreen computer cluster at the Joint Global Change Research Institute (JGCR) supported by the DOE Integrated Assessment Research Program. PNNL is operated for DOE by Battelle Memorial Institute under contract DE-AC05-76RL01830.

The Editor thanks two anonymous reviewers for their assistance in evaluating this paper.

#### References

- Chang, E. K. M., Y. Guo, and X. Xia (2012), CMIP5 multimodel ensemble projection of storm track change under global warming, *J. Geophys. Res.*, *117*, D23118, doi:10.1029/2012JD018578.
- Frierson, D. M. W., J. Lu, and G. Chen (2007), Width of the Hadley cell in simple and comprehensive general circulation models, *Geophys. Res. Lett.*, *34*, L18804, doi:10.1029/2007GL031115.
- Gao, Y., L. R. Leung, E. P. Salathé, F. Dominguez, B. Nijssen, and D. P. Lettenmaier (2012), Moisture flux convergence in regional and global climate models: Implications for droughts in the southwestern United States, *Geophys. Res. Lett.*, *39*, L09711, doi:10.1029/2012GL051560.
- Gent, P. R., et al. (2011), The Community Climate System Model version 4, *J. Clim.*, *24*(19), 4973–4991, doi:10.1175/2011JCLI4083.1.
- Ke, Y., L. R. Leung, M. Huang, A. M. Coleman, H. Li, and M. S. Wigmosta (2012), Development of high resolution land surface parameters for the Community Land Model, *Geosci. Model Dev.*, *5*(6), 1341–1362.
- Leung, L. R., and S. J. Ghan (1999), Pacific Northwest climate sensitivity simulated by a regional climate model driven by a GCM. Part II: 2xCO<sub>2</sub> simulations, *J. Clim.*, *12*(7), 2031–2053.
- Leung, L. R., Y. Qian, X. Bian, W. M. Washington, J. Han, and J. O. Roads (2004), Mid-century ensemble regional climate change scenarios for the western United States, *Clim. Change*, *62*(1), 75–113.
- Li, W., L. Li, M. Ting, and Y. Liu (2012), Intensification of Northern Hemisphere subtropical highs in a warmer climate, *Nat. Geosci.*, *5*(11), 830–834, doi:10.1038/NGEO1590.
- Lorenz, D. J., and E. T. DeWeaver (2007), Tropopause height and zonal wind response to global warming in the IPCC scenario integrations, *J. Geophys. Res.*, *112*, D10119, doi:10.1029/2006JD008087.
- Lu, J., G. A. Vecchi, and T. Reichler (2007), Expansion of the Hadley cell under global warming, *Geophys. Res. Lett.*, *34*, L06805, doi:10.1029/2006GL028443.
- Lu, J., G. Chen, and D. Frierson (2008), Response of the zonal mean atmospheric circulation to El Niño versus global warming, *J. Clim.*, *21*, 5835–5851.
- Maurer, E. P., A. W. Wood, J. C. Adam, D. P. Lettenmaier, and B. Nijssen (2002), A long-term hydrologically based dataset of land surface fluxes and states for the conterminous United States, *J. Clim.*, *15*(22), 3237.
- Mearns, L. O., et al. (2012), The North American Regional Climate Change Assessment Program: Overview of phase I results, *Bull. Am. Meteorol. Soc.*, *93*(9), doi:10.1175/BAMS-D-11-00223.1.
- Mearns, L. O., et al. (2013), Climate change projections of the North American Regional Climate Change Assessment Program (NARCCAP), *Clim. Change Lett.*, *120*(4), 965–975, doi:10.1007/s10584-013-0831-3.
- Moss, R. H., et al. (2010), The next generation of scenarios for climate change research and assessment, *Nature*, *463*, 747–756.
- Neelin, J. D., B. Langenbrunner, J. E. Meyerson, A. Hall, and N. Berg (2013), California winter precipitation change under global warming in the Coupled Model Intercomparison Project Phase 5 ensemble, *J. Clim.*, *26*(17), 6238–6256, doi:10.1175/JCLI-D-12-00514.1.
- Oleson, K. W., et al. (2010), Technical description of version 4.0 of the Community Land Model (CLM) NCAR/TN-478+STR. [Available at [www.cesm.ucar.edu/models/cesm1.0/clm/CLM4\\_Tech\\_Note.pdf](http://www.cesm.ucar.edu/models/cesm1.0/clm/CLM4_Tech_Note.pdf)].
- Pierce, D. W., et al. (2013), Probabilistic estimates of future changes in California temperature and precipitation using statistical and dynamical downscaling, *Clim. Dyn.*, *40*(3–4), 839–856, doi:10.1007/s00382-01201337-9.
- Seager, R., and G. A. Vecchi (2010), Greenhouse warming and the 21st century hydroclimate of southwestern North America, *Proc. Natl. Acad. Sci.*, *107*(50), 21,277–21,282.
- Seager, R., et al. (2007), Model projections of an imminent transition to a more arid climate in southwestern North America, *Science*, *316*(5828), 1181–1184.
- Seager, R., M. Ting, C. Li, N. Naik, B. Cook, J. Nakamura, and H. Liu (2013), Projections of declining surface-water availability for the southwestern United States, *Nature Clim. Change*, *3*(5), 482–486.
- Skamarock, W. C., J. B. Klemp, J. Dudhia, D. O. Gill, D. M. Barker, M. G. Duda, X. Huang, W. Wang, and J. G. Powers (2008), *A Description of the Advanced Research WRF Version 3*, NCAR Tech. Note, NCAR/TN-475+STR, 8 pp., Natl. Cent. for Atmos. Res., Boulder, Colo., U.S.A. [Available at [http://www.mmm.ucar.edu/wrf/users/docs/arw\\_v3.pdf](http://www.mmm.ucar.edu/wrf/users/docs/arw_v3.pdf)].
- Taylor, K. E., R. J. Stouffer, and G. A. Meehl (2012), An overview of CMIP5 and the experiment design, *Bull. Am. Meteorol. Soc.*, *93*(4), 485–498.
- Tebaldi, C., J. M. Arblaster, and R. Knutti (2011), Mapping model agreement on future climate projections, *Geophys. Res. Lett.*, *38*, L23701, doi:10.1029/2011GL049863.
- van Vuuren, D. P., et al. (2011), The representative concentration pathways: An overview, *Clim. Change*, *109*(1–2), 5–31, doi:10.1007/s10584-011-0148-z.